Suppression of itinerant ferromagnetism and cluster-glass behaviour of colossal magnetoresistive Ta-substituted $La_{0.67}Ca_{0.33}MnO_3$

2007 J. Phys.: Condens. Matter 19 216218

(http://iopscience.iop.org/0953-8984/19/21/216218)

IOP PUBLISHING JOURNAL OF PHYSICS: CONDENSED MATTER

J. Phys.: Condens. Matter **19** (2007) 216218 (22pp) doi:10.1088/0953-8984/19/21/216218

Suppression of itinerant ferromagnetism and cluster-glass behaviour of colossal magnetoresistive Ta-substituted $La_{0.67}Ca_{0.33}MnO_3$

L Seetha Lakshmi[1,2,3], K Dörr[2], K Nenkov[2], A Handstein[2], K-H Müller[2] and V S Sastry[1]

[1] XS & CGS, Materials Science Division, Indira Gandhi Centre For Atomic Research, Kalpakkam 603102, Tamil Nadu, India
[2] Institute of Metallic Materials, IFW Dresden, Postfach 270116, Dresden 01171, Germany

E-mail: slaxmi73@gmail.com

Received 29 December 2006, in final form 31 March 2007
Published 1 May 2007
Online at stacks.iop.org/JPhysCM/19/216218

Abstract

We discuss the modified magnetic state of single-phase $La_{0.67}Ca_{0.33}Mn_{1-x}Ta_xO_3$ ($x \leqslant 0.10$) colossal magnetoresistive compounds with orthorhombic *Pnma* symmetry. Pentavalent Ta substitution results in an extraordinarily strong reduction of the magnetic phase transition temperatures (∼39 K/at.%) in the ferromagnetic–metallic regime ($x \leqslant 0.03$) and suppresses the metal–insulator transition for $x \geqslant 0.05$. Many experimental features show evidence for the cluster-glass behaviour of the compounds with $x \geqslant 0.05$. These features are large thermomagnetic irreversibility just below the Curie temperature (T_c), monotonic increase of the field cooled magnetization down to 4.2 K, non-saturation of magnetization, and the observation of two distinct magnetic transitions in ac susceptibility in an appropriate dc field—one close to T_c and the other at a lower temperature (the spin-freezing temperature (T_g)). These results find additional support from non-equilibrium spin dynamics with a maximum in magnetic viscosity at T_g and a linear low-temperature magnetic specific heat with a characteristic broad maximum close to T_g.

1. Introduction

The (La, Ca)MnO_3 compounds belong to the class of strongly correlated electron systems, where the subtle balance between charge, orbital, lattice and spin degrees of freedom [1] results in a fascinating array of ground states with distinct physical properties [2]. The end members of the system are antiferromagnetic insulators [3], and their physical properties evolve as a function of hole doping. The currently accepted opinion is that the states of these manganites

[3] Author to whom any correspondence should be addressed.

are intrinsically inhomogeneous on different length scales. The competitive interactions due to various degrees of freedom drive the system to phase separate, involving mostly a ferromagnetic (FM) phase in the paramagnetic/antiferromagnetic charge-ordered insulating matrix [4]. Further, it has been argued in recent theoretical and experimental studies [5–8] that the stability of the ferromagnetic (metallic) phase and the occurrence of glassy ground states are affected by competing magnetic interactions in the background of quenched disorder.

In manganites, since the essential degrees of freedom are closely linked to the Mn ion, disorder effects controlling the stability of the FM phase can be manipulated by the substitutions at the Mn site. The chemical nature of the substituent has a crucial bearing on the magnetic properties of the compounds. For instance, paramagnetic substitutions, in addition to causing structural changes, bring out the additional complexity of local spin-coupling effects. On the other hand, diamagnetic isovalent substitutions are not expected to introduce any magnetic interactions of their own. In fact, previous reports showed that all possible Mn site substitutions of $La_{0.67}Ca_{0.33}MnO_3$, such as transition metal ions [9–18] or Al [19, 20], Ga [21], Ge [22], In [23] or Sn [24], lower the phase transition temperatures, but to different extents, and eventually lead to insulating states exhibiting glassy properties for higher substitutions. For instance, a cluster glass behaviour is reported in In-substituted [23] and Cu-substituted [25] $La_{2/3}Ca_{1/3}MnO_3$ compounds with $x \geqslant 0.05$. On the other hand, a spin-glass-like state at low temperatures is evidenced in $La_{2/3}Ca_{1/3}MnO_3$ substituted with Zn [26], Al [20], Sc [27], Ga [28], Ti [12], and Nb-substituted $La_{0.7}Sr_{0.3}MnO_3$ [29], but for still higher degree of substitution. At this point, it is important to recall that very similar results are also obtained for certain La-site substituted manganites such as $(La_{1-x}Gd_x)_{2/3}Ca_{1/3}MnO_3$ [10], $(La_{1-x}Tb_x)_{2/3}Ca_{1/3}MnO_3$ [30, 31] and $(La_{1-x}Dy_x)_{0.7}Ca_{0.3}MnO_3$ [32]. Terai *et al* [32] and Maignan *et al* [33] have established that not only the average ionic size of the La site ($\langle r_A \rangle$) or tolerance factor (t), but also La-site disorder (σ^2) effect, as suggested by Rodriguez-Martínez *et al* [34], plays an important role in controlling the magnetic ground state of those compounds. Recently, a system of $La_{0.7}Ca_{0.3}Mn_{1-x}Cd_xO_3$ ($0 \leqslant x \leqslant 0.2$) has drawn up an interesting picture that, depending on the Cd concentration, these materials exhibit a wide range of magnetic phases, such as the cluster-glass state for $x \geqslant 0.10$, but a spin-glass phase for $0.15 \leqslant x \leqslant 0.20$ composition [18]. Further, Al-doped charge-/orbital-ordered $Pr_{0.5}Ca_{0.5}MnO_3$ show that the thermal blocking of antiferromagnetic clusters of mesoscopic length scale leads to glassy states in those compounds [35]. The nature of the low-temperature magnetic state of Mn-site substituted compounds with paramagnetic ions were also intensively studied. For instance, Co substitution in $La_{0.7}Ca_{0.3}MnO_3$ leads to a cluster-glass phase from the usual long-range ferromagnetic state [11]. Cr substitution in $La_{2/3}Ca_{1/3}MnO_3$, on the other hand, suppresses the usual long-range ferromagnetism and induces spin-glass-like behaviour at low temperatures [36]. Similarly, a spin-glass-type of behaviour with spin-freezing temperature of 42 K has been reported by Cai *et al* for the $La_{0.67}Ca_{0.33}Mn_{0.90}Fe_{0.10}O_3$ compound [37]. However, neutron depolarization results do not support the spin-glass state of that compound. Unlike the case of a true spin-glass state where no depolarization is expected, the Fe-substituted compound shows significant depolarization of the transmitted beam of neutrons down to 15 K, and this confirms the coexistence of clusters of spins with net magnetic moment in mesoscopic length scales [38]. An inconsistency in the results of Cai *et al* [37] was the fact that they correlated the broad maximum in the resistivity around 42 K with the spin-freezing temperature. However, a double-exchange mediated spin glass should be insulating, as observed, for instance, in $(La_{2/3}Tb_{1/3})_{2/3}Ca_{1/3}MnO_3$ [31].

From the preceding discussions, it is inferred that a glassy phase exhibiting a variety of relaxation and ageing effects, possibly arising due to phase competitions, is a phenomenon far more common in certain manganites. But whether the glassy phase mimics the canonical

spin glasses, super-paramagnets and/or cluster glasses or whether phase segregation in these materials leads to a new form of glassy phase remains to be understood [39]. This is one of the challenging research problems of current interest. Rigorous experimental and computational studies are underway, and many more exciting results are expected in the near future. In our previous studies on Mn-site substitutions with both diamagnetic and paramagnetic isovalent ions, it was shown that there are two important contributions, namely local structure and local spin-coupling effects, that control the phase transition temperatures and stability of the ferromagnetic–metallic (FM–M) ground state of colossal magnetoresistive (CMR) manganites [40]. It was also hypothesized that local ferromagnetic coupling partially compensates the local structural effects, leaving the ferromagnetic–metallic phase intact over a relatively wide range of substitution [41]. However, the non-isovalent diamagnetic substitutions introduce more drastic effects. Our recent studies with non-isovalent diamagnetic ions, such as divalent Zn, tetravalent Zr, pentavalent Ta and hexavalent W, show that higher valence state substituents reduce the phase transition temperatures more strongly compared to their isovalent counterpart at the Mn site of $La_{0.67}Ca_{0.33}MnO_3$ system. These studies unequivocally establish the fact that charge-state modification plays an aggressive role, compared to local structure and local coupling effects, for the unusually strong reduction of the phase transition temperatures and itinerant ferromagnetism in the CMR manganites [42].

In this context, it is important to note that pentavalent Ta substitution in $La_{0.67}Ca_{0.33}MnO_3$ suppresses the ferromagnetic–metallic ground state for $x \geqslant 0.05$ [43]. In this paper, we report the nature of the modified magnetic state of the substituted compounds. A detailed discussion of the crystal structure and magneto-transport properties is being published elsewhere [42]. Ta-substituted compounds beyond $x = 0.03$ are chosen for the dynamic and static studies. Under dynamic response, relaxation measurements at selected temperatures and the ac susceptibility measurements, with excitation frequency varied over three decades, both in the absence and the presence of suitable static bias fields, are carried out. Under static response, zero-field-cooled (ZFC) and field-cooled (FC) thermomagnetization measurements and magnetization under sweep field are performed. Dynamic and static magnetic responses of the system provide a strong indication of a cluster-glass-like state of the system. These observations find additional support from specific heat studies under zero field of $x = 0.10$, the highest substitution level of the present study.

2. Experimental details

Bulk polycrystalline samples, $La_{0.67}Ca_{0.33}Mn_{1-x}Ta_xO_3$ ($0 \leqslant x \leqslant 0.10$), were prepared by solid-state reaction according to the procedure described in our earlier work [42]. The high statistics room-temperature (RT) powder x-ray diffraction (XRD) patterns were recorded in the 2θ range, 15°–120° using Cu Kα radiation and a STOE diffractometer. The lattice parameters and unit cell volume were estimated using the GSAS Rietveld refinement program [44] and SPUDS program [45] to generate a starting model for the Rietveld analysis. The temperature variation of resistivity ($\rho(T)$) in four-probe linear geometry was carried out using a MAGLAB^{1992} system (Oxford Instruments, UK). A split-coil superconducting magnet was employed to produce a steady magnetic field $\leqslant$7 T with the magnetic field applied parallel to the current direction. The temperature variation of ac susceptibility under an ac probe field (h) of 1 Oe and an excitation frequency (f) of 133 Hz was recorded using a Lakeshore 7000 series ac susceptometer. The effect of static bias field and excitation frequency on the ac susceptibility was investigated in ZFC condition using a physical property measurement system (PPMS) (Quantum Design, USA, Model: 6000). The static field (H) and excitation frequency of the probe field were varied in the ranges 0–3 kOe and 133 Hz–

10 kHz, respectively. The ZFC and FC thermomagnetization ($M_{ZFC}(T)$ and $M_{FC}(T)$) as a function of applied field (H), field-dependent magnetization ($M(H)$) and time-dependent decay of thermoremanent magnetization ($M(t)$) at selected temperatures were recorded using a commercially available SQUID magnetometer (MPMS-5, Quantum Design, USA). Magnetic relaxation data at different preselected temperatures were acquired in the following sequence. The sample was cooled from the reference temperature (T_{ref}) of 275 K in a constant magnetic field of 10 mT to the desired temperature. At this temperature, a waiting time (t_w) of 600 s was given before the field was switched off and the decay of remanent magnetization was recorded as a function of elapsed time over three decades (∼4000 s). After the data collection, the sample was heated to T_{ref} in ZFC condition to remove the history-dependent effects. The analysis of the decay is described in section 3.5.

The specific heat (C_p) measurements were performed by relaxation calorimetry in heat pulse mode, using the PPMS. The performance of the set up, prior to the data collection, was checked with standard copper, and the accuracy was found to be better than 2%. The sample, in the form of thin slabs (0.4 mm × 0.8 mm × 5 mm) weighing about 50 mg, was mounted on the sapphire disc using Apiezon grease. The mass of the grease was kept to a minimum (∼0.2 mg) and was weighed accurately, in order to subtract its contribution to the total heat capacity. The sample was cooled in ZFC condition from 300 to 1.9 K and the data were recorded in the warming mode. A two-tau model [46] was used to fully automate the analysis of the raw data and the subtraction of the addentum heat capacity which was recorded separately. The C_p data are analysed in section 3.6.

The Curie temperature (T_c) corresponding to the onset of the in-phase component of the ac susceptibility (χ') signal was estimated by a tangent method. The spin-freezing temperature (T_g) is denoted as the temperature corresponding to the low-temperature maximum in the in-phase component of the static field biased ac susceptibility ($\chi'(T; H)$). The temperature at which $M_{ZFC}(T)$ and $M_{FC}(T)$ for a given measuring field (H) start to bifurcate is represented as the temperature of irreversibility (T_{irr}).

3. Experimental results

3.1. Structural properties

The entire powder x-ray diffraction pattern of polycrystalline $La_{0.67}Ca_{0.33}Mn_{1-x}Ta_xO_3$ ($0 \leqslant x \leqslant 0.10$) compounds could be indexed to orthorhombic *Pnma* space group (space group No. 62) [43]. Rietveld refinement yielded an excellent agreement between the observed (I_{obs}) and calculated (I_{cal}) diffraction profiles with no peaks are left unindexed, confirming the fact that the compounds are single phase [42]. As a representative of each series, the Rietveld-fitted x-ray diffraction patterns of $La_{0.67}Ca_{0.33}Mn_{1-x}Ta_xO_3$ ($x = 0$, 0.05 and 0.10) are displayed in figure 1.

The lattice parameters a, b and c and average Mn–O ($\langle d_{Mn-O}\rangle$) distance show a linear increase with Ta substitution; hence an overall linear expansion of the unit cell is observed [43]. On the other hand, the average Mn–O–Mn bond angle shows a considerable decrease in the entire range of substitution. More detailed analysis and discussion of the crystal structure is being published elsewhere [42]. Taking charge neutrality into account, Ta^{5+} strongly shifts the average valence state of Mn towards 3+ according to $La^{3+}_{0.67}Ca^{2+}_{0.33}Mn^{3+}_{(0.67+x)}Mn^{4+}_{(0.33-2x)}Ta^{5+}_{x}O^{2-}_{3}$. It is important to note that Ta^{5+} not only decreases the Mn^{4+} concentration, but also increases the Mn^{3+} concentration. A close agreement is seen between relative Mn^{3+} and Mn^{4+} concentration estimated from the refinement program and the one predicted based on the charge-neutrality consideration [42]. The shift of average valence state of Mn ion to 3+ is expected to bring out an increase in the average Mn ionic radius

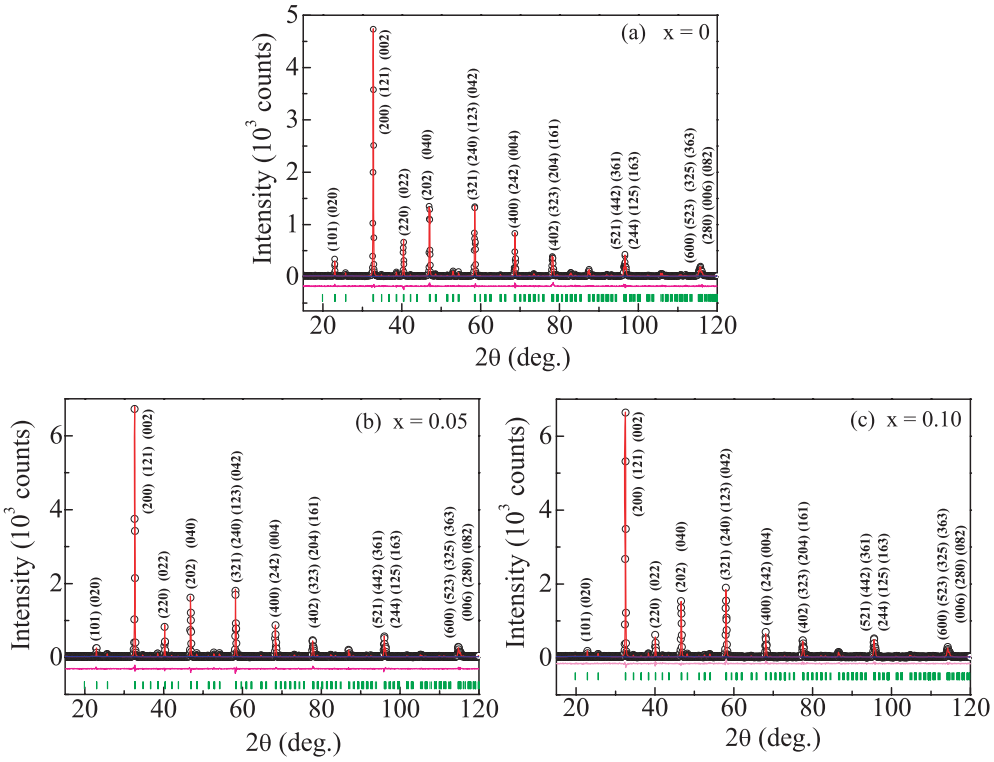

Figure 1. Rietveld refinement spectra of $La_{0.67}Ca_{0.33}Mn_{1-x}Ta_xO_3$ compounds where (a) $x = 0$, (b) 0.05 (c) 0.10. In each spectrum, the symbol denotes the observed intensity (I_{obs}), and the continuous line denotes the calculated intensity (I_{cal}). The difference between the observed and the calculated intensities is shown at the bottom of the figure. The calculated Bragg-reflected positions are marked by the vertical bars. The Miller indices of the major Bragg reflections are also indicated.

(This figure is in colour only in the electronic version)

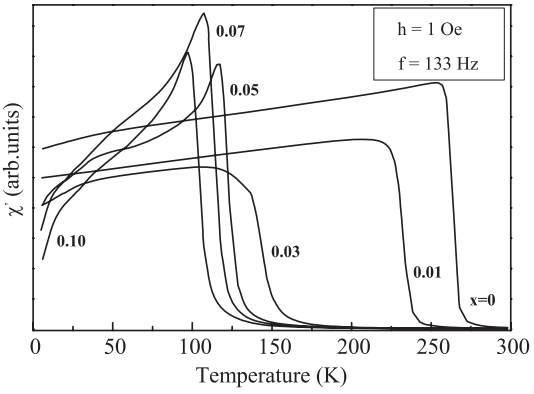

Figure 2. Temperature variation of in-phase component of ac susceptibility ($\chi'(T)$) measured in an ac probe field (h) of 1 Oe and at a frequency (f) of 133 Hz of $La_{0.67}Ca_{0.33}Mn_{1-x}Ta_xO_3$ ($0 \leqslant x \leqslant 0.10$) compounds.

($\langle IR_{Mn} \rangle$) and associated increase in the lattice parameters. Further, thermogravimetry studies show that the oxygen stoichiometry of all the compounds is close to the nominal composition of 3, and is expected not to influence the physical properties of the compounds [42].

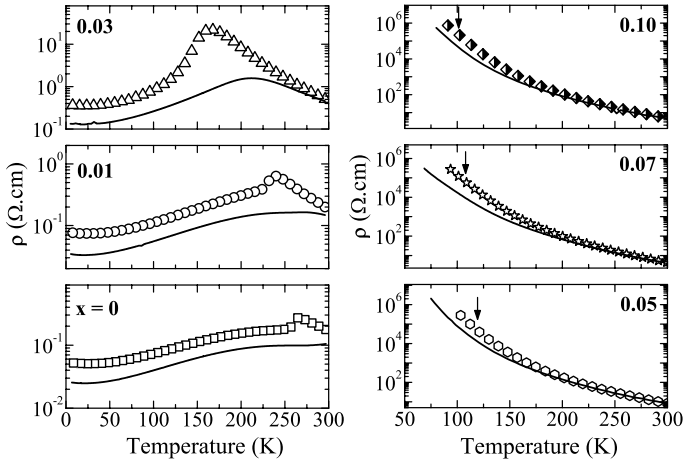

Figure 3. Temperature variation of resistivity ($\rho(T)$) in the absence of magnetic field (symbols) and in the presence of 7 T (continuous line) of $La_{0.67}Ca_{0.33}Mn_{1-x}Ta_xO_3$ ($0 \leqslant x \leqslant 0.10$) compounds. The arrow (right panel) indicates the Curie temperature in $\chi'(T)$ shown in figure 2.

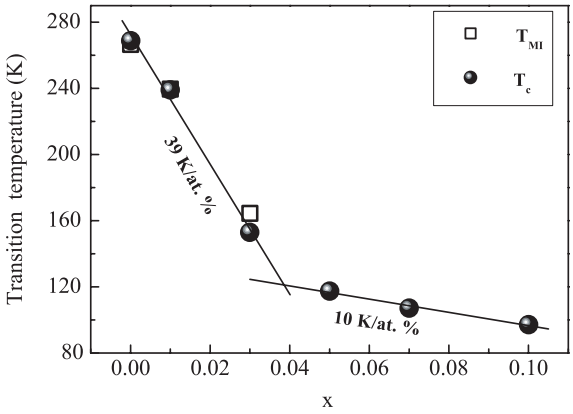

Figure 4. Variation of metal–insulator transition temperature (T_{MI}) and Curie temperature (T_c) as a function of x of $La_{0.67}Ca_{0.33}Mn_{1-x}Ta_xO_3$ ($0 \leqslant x \leqslant 0.10$) compounds. Straight lines are best fits to the experimental data to estimate the rate of suppression in the transition temperatures (dT_c/dx and dT_{MI}/dx).

3.2. Compositional dependence of phase transition temperatures (T_c and T_{MI})

As shown in figure 2, all the substituted compounds undergo a Curie transition at T_c. The T_c closely matches with the respective metal–insulator transition temperature (T_{MI}) for $x \leqslant 0.03$, and beyond this, the compounds exhibit an insulating behaviour with no perceptible anomaly near T_c (figure 3) indicating the non-metallic behaviour of the ferromagnetic phase [43]. The variation of T_c with the concentration of the substituent is nonlinear (figure 4): there is an initial strong decrease up to $x = 0.03$ ($dT_c/dx \approx dT_{MI}/dx \sim 39$ K/at.%) which levels off to a much smaller rate ($\sim$10 K/at.%) for higher Ta concentration. Another striking feature for $x > 0.03$ is the presence of a cusp-like feature in $\chi'(T)$ just below T_c and a broad shoulder at lower temperatures. These results, as will be discussed in the following, indicate that Ta substitution modifies the ground state to a cluster-glass insulator.

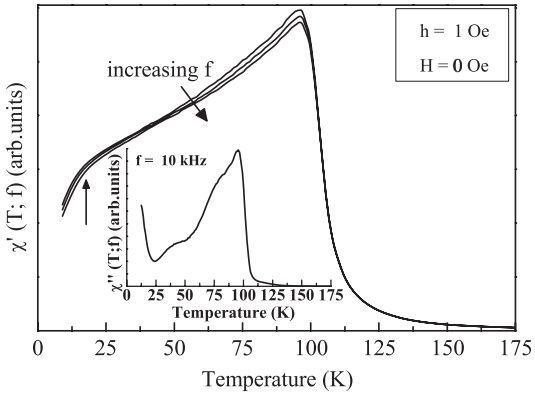

Figure 5. Temperature dependence of in-phase component ($\chi'(T; f)$) of the ac susceptibility of the $La_{0.67}Ca_{0.33}Mn_{0.90}Ta_{0.10}O_3$ compound in the absence of static bias field and at frequencies f of 0.133, 1 and 10 kHz and with an ac probe field (h) of 1 Oe. ↑ marks the broad shoulder in the $\chi'(T; f)$. The inset shows the out-of-phase component of the ac susceptibility ($\chi''(T; f)$) at $f = 10$ kHz.

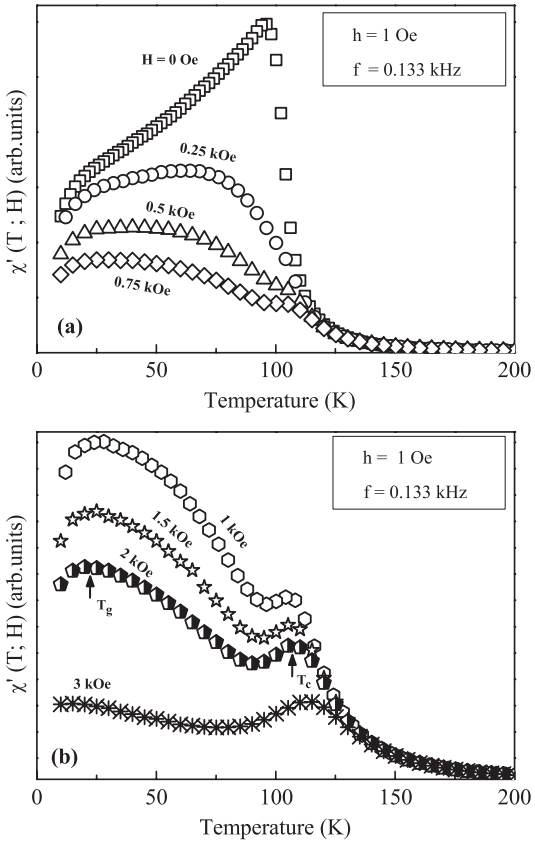

Figure 6. (a) and (b) Temperature dependence of the in-phase component of the ac susceptibility ($\chi'(T; H)$) of the $La_{0.67}Ca_{0.33}Mn_{0.90}Ta_{0.10}O_3$ compound measured in different applied static magnetic fields (□, ○, △, ◇, ⬡, ☆, ◑, and ✳, denote 0, 0.25, 0.5, 0.75, 1, 1.5, 2 and 3 kOe respectively) in an ac probing field (h) of 1 Oe and at a frequency f of 0.133 kHz. T_c and T_g denote the ferromagnetic and spin-freezing temperature respectively.

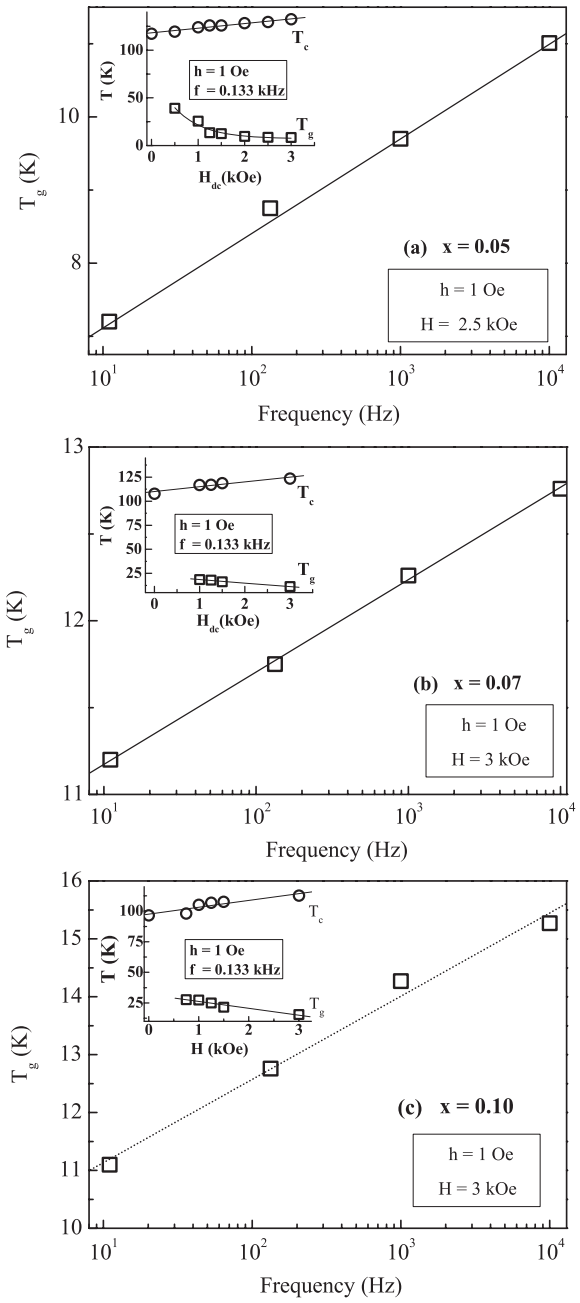

Figure 7. Frequency dependence of the freezing temperature (T_g) of $La_{0.67}Ca_{0.33}Mn_{1-x}Ta_xO_3$ compounds for (a) $x = 0.05$ (b) $x = 0.07$ and (c) $x = 0.10$. The inset shows the variation of Curie temperature (T_c) and T_g with static bias field.

3.3. Dynamic response

Dynamics studies involve ac susceptibility measurements of the Ta-substituted compounds beyond $x = 0.03$ using an ac probe field (h) of 1 Oe with excitation frequency (f) varied

over three orders, both in the absence and the presence of suitable static bias fields. The out-of-phase component, χ'' (absorption part), of the ac susceptibility shows a characteristic maximum corresponding to the additional features in the $\chi'(T)$ curves shown in figure 2. As a typical case, $\chi'(T)$ at $f = 10$ kHz will be discussed in the following. The χ'' signal becomes weak at lower temperatures as it is overwhelmed by noise, especially for the lower excitation frequencies of the ac probe field, precluding a detailed analysis to be carried out. The details of the dynamic response of the system are, therefore, unfortunately limited to the dispersion part (χ') of the ac susceptibility.

As a representative of the series, the temperature dependence of χ' of $x = 0.10$ under different excitation frequencies ranging from 0.133 to 10 kHz ($\chi'(f, T)$) for $h = 1$ Oe is shown in figure 5. All the curves retain the cusp-like anomaly just below T_c and a broad shoulder at lower temperatures. It is important to note that the position of the cusp-like anomaly is frequency independent. Only in the region close to and below the cusp-like anomaly, could a notable suppression of the χ' signal with increasing frequency be seen. The static field dependence of the ac susceptibility ($\chi'(T; H)$) in fields up to 3 kOe under an excitation frequency of 0.133 kHz is shown in figure 6. Suppression of the χ' maximum and broadening of the anomaly is observed for $H_{dc} = 250$ Oe (figure 6(a)). At much higher fields, two separate maxima could be observed (figure 6(b)). While the high-temperature peak broadens and shifts to higher temperatures, the low-temperature peak shifts to low temperatures with an increase in the bias field (inset of figure 7(c)). Such opposing shifts are observed for $x = 0.05$ and 0.07 as well (inset of figures 7(a) and (b)). Figure 8 shows the effect of frequency on the ac susceptibility ($\chi'(T; H; f)$) under a static bias field of 3 kOe for $x = 0.10$. The high-temperature maximum is quite insensitive to the frequency in terms of signal strength and its position. On the other hand, a distinct frequency dependence of the low-temperature maximum and the suppression of the χ' signal at lower temperatures were observed. It is clearly seen that the low-temperature maximum (T_g) shifts to higher temperature on increasing the frequency. The dependence of its peak position with applied frequency is depicted in figure 7(c). As shown in figure 7(c), the frequency dependence of T_g follows a straight line. The fractional shift of T_g per decade of frequency, i.e., $p = \Delta T_g/[T_g \Delta(\log_{10} f)]$, is estimated from the slope of the $\log_{10} f$ versus $1/T_g$ curves, and a typical value is estimated to be ~0.22.

3.4. Static studies

3.4.1. ZFC and FC thermomagnetization under different H. ZFC and FC thermomagnetization ($M(T)$) curves of the $La_{0.67}Ca_{0.33}Mn_{0.90}Ta_{0.10}O_3$ compound, as a representative of the series, measured under an applied magnetic field of 0.01, 0.1 and 1 kOe, are displayed in figures 9(a)–(c) respectively. The paramagnetic to ferromagnetic transition temperature, as determined from the inflection point, is estimated to be ~110 K, and this is in accordance with the value of T_c determined from the χ' curves (figure 2). The transition becomes broad and shifts to higher temperature with an increase of applied field. The $M_{ZFC}(T)$ curves recorded under $H = 0.01$ kOe show a shallow maximum at about $T_p \sim 91$ K, whereas such a feature is absent in the $M_{FC}(T)$ curves. The $M_{ZFC}(T)$ and $M_{FC}(T)$ curves start to bifurcate below the temperature of irreversibility (T_{irr}). The M_{FC} signal and therefore $\Delta M = (M_{FC} - M_{ZFC})/M_{ZFC}$ continue to increase below T_{irr} until the lowest temperature of measurement (4 K). With the increase of the applied field, the shallow maximum becomes shallower with a decrease in the value of T_p, T_{irr} and ΔM.

3.4.2. Field dependence of magnetization. The field-dependent magnetization of the $La_{0.67}Ca_{0.33}Mn_{0.90}Ta_{0.10}O_3$ compound was measured in ZFC condition at 100 K ($\approx T_c$) and

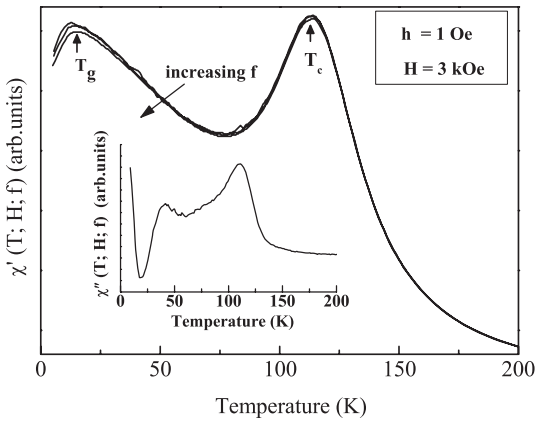

Figure 8. Temperature dependence of the in-phase component of the ac susceptibility ($\chi'(T; H; f)$) of the $La_{0.67}Ca_{0.33}Mn_{0.90}Ta_{0.10}O_3$ compound measured at f of 0.133 and 1 and 10 kHz in a static magnetic field of 3 kOe and an ac probe field of 1 Oe. The inset shows the out-of-phase component of the ac susceptibility ($\chi''(T; H; f)$) at $f = 10$ kHz.

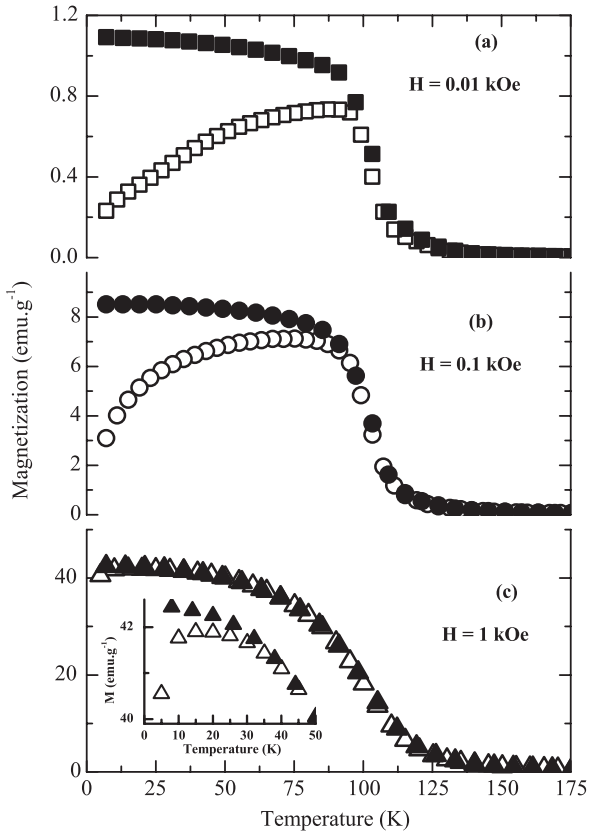

Figure 9. ZFC (open symbols) and FC (closed symbols) thermomagnetization ($M(T)$) curves of the $La_{0.67}Ca_{0.33}Mn_{0.90}Ta_{0.10}O_3$ compound for H of (a) 0.01, (b) 0.1 and (c) 1 kOe. The inset of figure 8(c) shows the $M(T)$ curve below 50 K for $H = 1$ kOe on an enlarged scale.

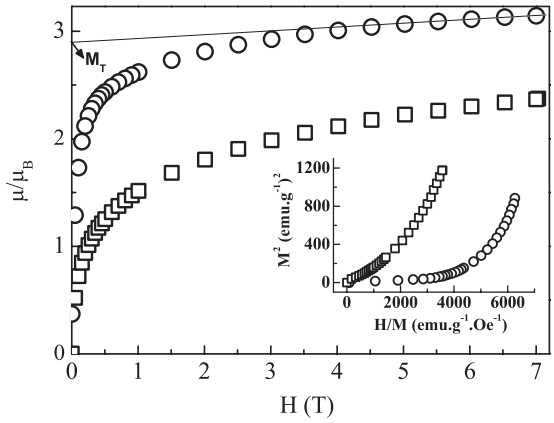

Figure 10. Field dependence of magnetization of the $La_{0.67}Ca_{0.33}Mn_{0.90}Ta_{0.10}O_3$ compound measured in ZFC condition at selected temperatures of 100 (○) and 5 K (□). M_T marks the residual slope of the technical saturation. The Y axis is normalized to magnetic moment per formula unit per Bohr magneton (μ/μ_B). The inset shows the Arrot plot of the compound at 100 and 5 K.

Table 1. Best-fit parameters to the exponential decay (equation (2)) for the data in figure 11(g).

	T (K)	
Parameters	70	90
M_0 (emu g^{-1})	0.8661 ± 0.0001	0.4901 ± 0.0001
M_1 (emu g^{-1})	0.0192 ± 0.0006	0.0112 ± 0.0002
M_2 (emu g^{-1})	0.0123 ± 0.0005	0.0060 ± 0.0002
τ_1 (s)	93.39 ± 5.16	78.42 ± 3.00
τ_2 (s)	865.58 ± 64.03	827.73 ± 47.64

5 K with a maximum magnetic field of 7 T, and is presented in figure 10. It is seen that at both temperatures the saturation of magnetization is not achieved up to the maximum sweep field of 7 T. The magnetic moment per Mn ion as calculated from the technical saturation (marked as M_T in figure 10) is $\sim$2.86 μ_B.

3.5. Relaxation studies

The time decay of remanent magnetization ($M(t)$) in the temperature range 5–90 K of the $La_{0.67}Ca_{0.33}Mn_{0.90}Ta_{0.10}O_3$ compound, as a representative of the series, is shown in figure 11. The relaxation effect with no saturation in the timescale of the measurements is seen at all temperatures. Various functional forms, such as power law [47, 48], stretched exponential [49], logarithmic decay [50, 51], etc, are frequently invoked in the analysis of compounds showing glassy behaviour. However, in the present case, a single functional form fails to fit the decay curves over the entire temperature range of measurement. A trial and error fitting procedure covering the entire time window ($t \leqslant 4000$ s) shows that the relaxation isotherms of the compound need to be grouped into two distinct thermal regimes, $T < 70$ K and $T > 70$ K.

3.5.1. $T < 70$ K. In this temperature regime, the decay of $M(t)$ in the entire time window can be described well by a logarithmic decay of the functional form [52]

$$M(t) = M_0[1 - S\ln(1 + t/t_0)] \tag{1}$$

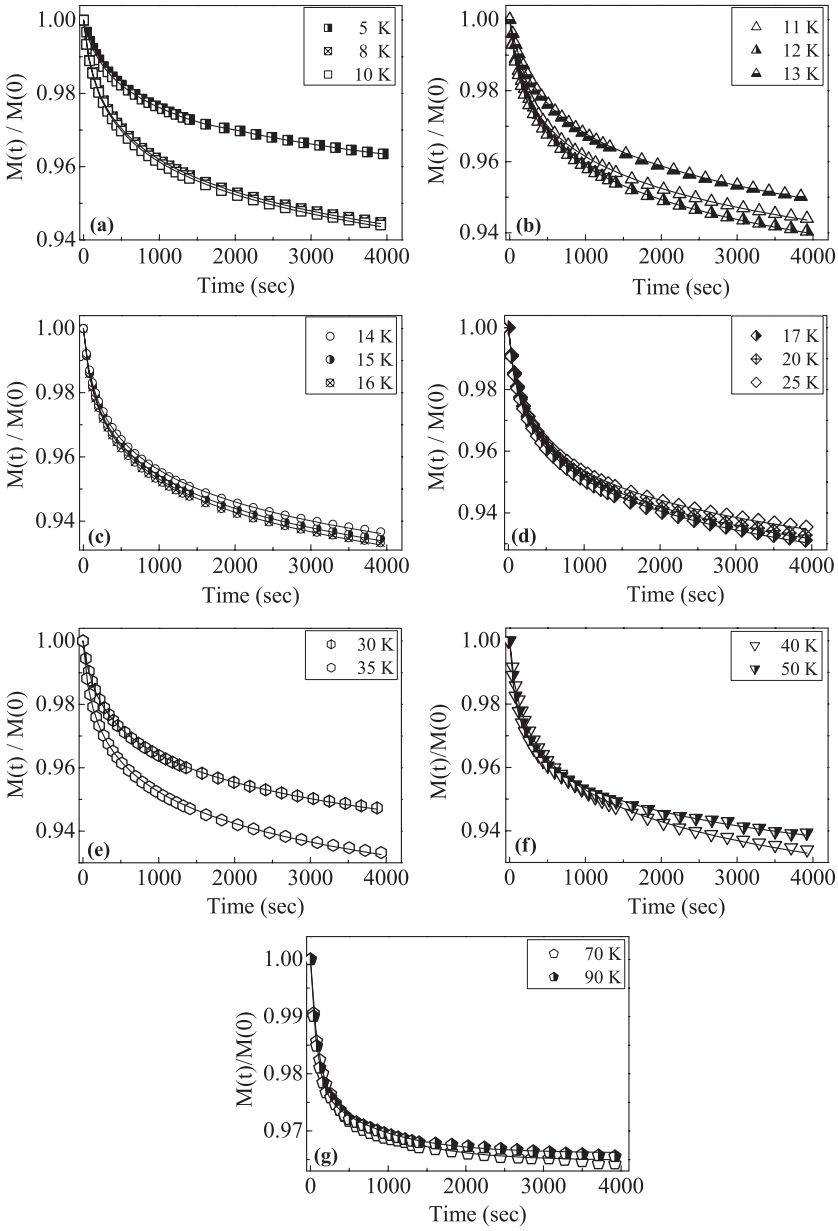

Figure 11. (a)–(g) Thermoremanent relaxation isotherms of the $La_{0.67}Ca_{0.33}Mn_{0.90}Ta_{0.10}O_3$ compound after cooling the sample from 250 K to different temperatures in a field of 10 mT and switching off the field at $t = 0$ after a waiting time of t_w of 600 s. The solid line is the best fit to the experimental data to equation (1) for $T < 70$ K and to equation (2) for $T \geqslant 70$ K.

where M_0 is the initial remanent magnetization, S is the magnetic viscosity that depends on the magnetic field, temperature and material, and t_0 is a reference time which depends on the sample and measuring procedure. It is interesting to note that $S(T)$ exhibits two maxima; one at ∼40 K and another at ∼20 K (figure 12).

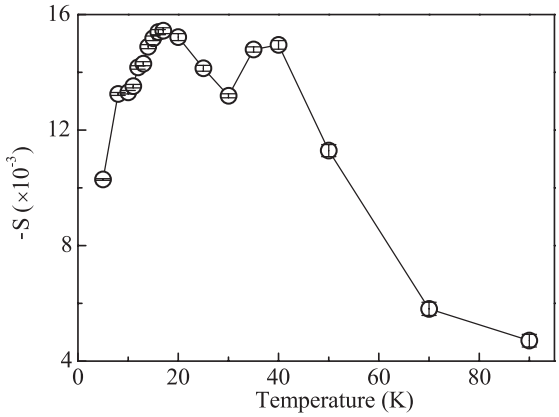

Figure 12. Temperature dependence of magnetic viscosity ($S(T)$) of the $La_{0.67}Ca_{0.33}Mn_{0.90}Ta_{0.10}O_3$ compound.

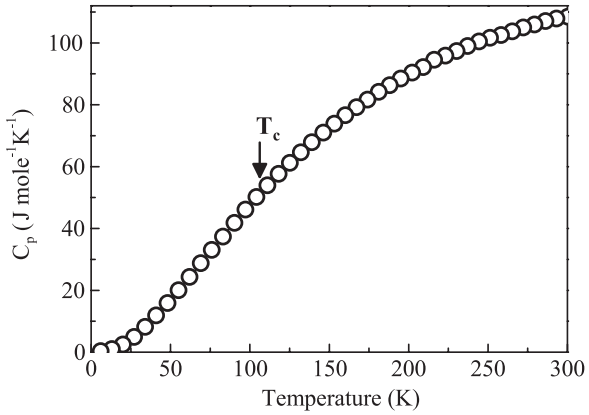

Figure 13. Temperature dependence of specific heat ($C_p(T)$) of the $La_{0.67}Ca_{0.33}Mn_{0.90}Ta_{0.10}O_3$ compound in ZFC condition. The arrow refers to the Curie temperature (T_c) determined from the ac susceptibility.

3.5.2. $T \geqslant 70$ K. In this temperature regime, the decay of $M(t)$ could no longer be fitted to logarithmic decay but only to exponential decay (Debye-exponential). However, a single exponential decay function could not be fitted to entire time window, and the best fit was a sum of two exponential decay terms [53] given by

$$M(t) = M_0 + M_1 e^{-t/\tau_1} + M_2 e^{-t/\tau_2} \tag{2}$$

where M_0 relates to an intrinsic ferromagnetic component and M_1 and M_2 to a glassy component mainly contributing to the observed relaxation effects, and τ_1 and τ_2 are closely associated with the response time. Corresponding fitted values are tabulated in table 1.

3.6. Specific heat

Figure 13 displays the variation of specific heat with temperature ($C_p(T)$) of the $La_{0.67}Ca_{0.33}Mn_{0.90}Ta_{0.10}O_3$ compound. Unlike the undoped compound [54] or lightly doped manganites [14, 55], no distinct anomaly is observed corresponding to T_c. Similar observations

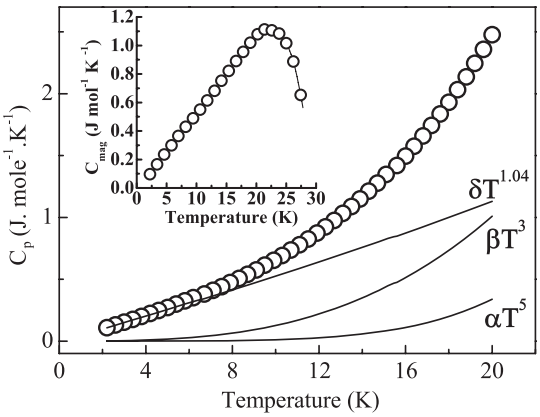

Figure 14. Specific heat ($C_p(T)$) of the $La_{0.67}Ca_{0.33}Mn_{0.90}Ta_{0.10}O_3$ compound in the low-temperature range (2–20 K). The solid lines are various contributions to C_p (see text). The inset shows the temperature variation of the magnetic contribution to the total specific heat ($C_{mag}(T)$) of the $La_{0.67}Ca_{0.33}Mn_{0.90}Ta_{0.10}O_3$ compound obtained after subtracting the lattice contribution to the total specific heat.

Table 2. Summary of fitting results for the data in figure 14 to equation (3). The units of different quantities are β (J mol^{-1} K^{-4}), α (J mol^{-1} K^{-6}), δ (J mol^{-1} K^{-2}) and θ_D (K).

Parameter	Value
β	$0.000\,13 \pm 5.04 \times 10^{-6}$
α	$1.113 \times 10^{-7} \pm 7.4 \times 10^{-9}$
δ	$0.04768 \pm 9.4 \times 10^{-5}$
n	1.04 ± 0.01
θ_D	447.35 ± 5.89

have also been reported for Fe-substituted ($x \geqslant 0.07$) [55], Ga-substituted ($x \sim 0.10$) [56] and Zn-substituted ($x \geqslant 0.15$) [14] manganites. The total specific heat of the system [57] is given by

$$C_p(T) = C_{p(\text{hyper})} + C_{p(\text{elec})} + C_{p(\text{latt})} + C_{p(\text{mag})} \tag{3}$$

where $C_{p(\text{hyper})} = A/T^2$ is the hyperfine contribution caused by the local magnetic field at the Mn nucleus due to the electrons in unfilled shells, $C_{p(\text{elec})} = \gamma T$ is the electronic contribution due to free electrons, $C_{p(\text{lattice})} = \beta T^3 + \alpha T^5$ is the approximate lattice contribution at low temperature and $C_{p(\text{mag})} = \delta T^n$ is the spin-wave contribution. The value of n depends on the nature of excitations: for a standard Néel antiferromagnet (AFM), $n = 3$; for an A-type AFM such as $LaMnO_3$, $n = 2$ [58]; for a ferromagnet, spin-wave excitation yields $n = 3/2$ [57]; and approximately linear temperature dependence is observed for spin-glass systems [59–61].

With a view to extracting the magnetic contribution, C_p in the low-temperature range (2–20 K) is fitted to equation (3) and is shown in figure 14. No upturn in C_p at low temperature indicates the absence of a hyperfine contribution to C_p that accordingly was omitted in the analysis. First, the data were fitted using all other terms and floating all the parameters. This resulted in unphysical values of the parameters α, β and γ. In the next step n was set to 1.5, but no improvement in the fitting could be seen. We then tried to fit the data using different assumptions such as setting one or two parameters equal to zero. By employing different combinations in the fitting procedures, an excellent fit was obtained when $C_{p(\text{elec})}$ was set to

zero. Since the compound is an insulator under a magnetic field of 7 T at 5 K (figure 3) it is quite physical to assume that the free-electron contribution to C_p is negligible. Thus, for this compound and in the temperature interval 2–20 K, $C_{p(\text{latt})}$ and $C_{p(\text{mag})}$ alone contribute to C_p. The fitted parameters are listed in table 2. Under this fitting procedure, the Debye temperature (θ_D) is estimated to be ~447 K from the relation $\theta_D = (12\pi^4 pR/5\beta)^{1/3}$, where R is the gas constant and p (=6) is the number of atoms per unit cell [57]. This θ_D value is in agreement with the reported values for the manganites [58, 62]. The fitting yields a value of 1.04 ± 0.01 for n, indicating a linear contribution. The magnetic specific heat (C_{mag}) as a function of temperature obtained by subtracting the phonon contribution is shown in the inset of figure 14.

4. Discussion

We first discuss the static response of $La_{0.67}Ca_{0.33}Mn_{0.90}Ta_{0.10}O_3$ under different magnetic fields. The magnetization has history dependence with a bifurcation between $M_{\text{ZFC}}(T)$ and $M_{\text{FC}}(T)$ below the irreversibility temperature, T_{irr} (figure 9). When the applied field is 0.01 kOe, $M_{\text{ZFC}}(T)$ displays a broad cusp-like anomaly at a temperature just below T_c and a sharp drop of the magnetization at a lower temperature. $M_{\text{FC}}(T)$ registers a steep increase near T_c followed by a weak temperature-dependent increase down to 4.2 K. The qualitative behaviour of the magnetization changes with increasing field, i.e., the maximum in M_{ZFC} seen at low fields, loses its sharpness and becomes a broad maximum. $M_{\text{ZFC}}(T)$ shows a monotonic increase and the drop of magnetization decreases with increasing field. Consequently, the thermomagnetic irreversibility decreases and both T_p and T_{irr} shift to lower temperature with the increase of field up to 1 kOe (figure 15). Thus, the system exhibits a paramagnetic to ferromagnetic transition and spin freezing at still lower temperature, implying that the ground state is a glassy state. Such a two-transition behaviour, namely, T_c followed by spin freezing, is exhibited by re-entrant spin-glass (RSG) [63] and cluster-glass (CG) systems [64–66]. We note that the $M_{\text{FC}}(T)$ signal continues to increase with decreasing temperature below T_{irr}. This may be recognized as a typical feature of the various CG systems [67–69]. It should, however, be recalled that M_{FC} of a canonical spin-glass is almost temperature independent below T_{irr} [70–73]. Also $T_{\text{irr}} \ll T_c$ for RSG systems such as NiMn [74, 75], AuFe [76] and FeZr [77], whereas for a CG system, T_{irr} is just below T_c, as observed in $La_{0.5}Sr_{0.5}CoO_3$ [78]. Non-saturation of the thermomagnetization below T_{irr} (figure 10) and $T_{\text{irr}} \sim T_c$ (figure 9) clearly indicate that the low-temperature state of the Ta-substituted $La_{0.67}Ca_{0.33}MnO_3$ compound is CG. The T_c observed here, as will be shown subsequently, is associated with the clusters themselves. Additional information on these clusters could be obtained from the thermomagnetization by considering two parameters, the relative history dependence of magnetization at 5 K, $\Delta M = (M_{\text{FC}} - M_{\text{ZFC}})/M_{\text{ZFC}}$ [79] and the difference between T_{irr} and T_p (ΔT) (figure 15). For $H = 0.01$ kOe, the magnetization is strongly dependent on the magnetic history in that ΔM is comparatively large. Such a strong dependence suggests that inter-cluster interactions dominate over the effects of the external magnetic field of 0.01 kOe. The relatively smaller value of ΔT indicates that the ferromagnetic clusters in these low fields are uniform in size [80]. When $H = 0.1$ kOe, no significant decrease is observed for T_{irr}. On increasing the field, ΔT rises sharply and ΔM drops to an appreciable extent. An increase in ΔT is expected to arise from a wider size distribution of the clusters [81]. Moreover, the magnetization curves measured as function of field do show the signature of the glassy ground state. It is apparent that no saturation of magnetization is achieved even up to a field of 7 T and at a temperature as low as 5 K (figure 10), supporting the idea of the CG ground state. The value of magnetic moment per Mn ion of 2.86 μ_B is much smaller than the

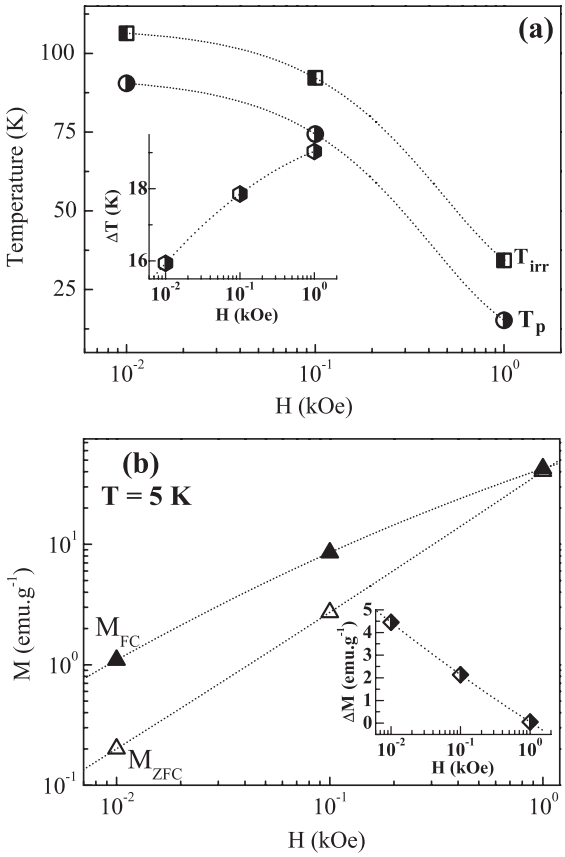

Figure 15. The field dependence of (a) the temperature of the maximum in $M_{\mathrm{ZFC}}(T)$, (T_{p}) and irreversibility temperature (T_{irr}), and the difference between T_{irr} and T_{p} $\Delta T = T_{\mathrm{irr}} - T_{\mathrm{p}}$ (◑) (inset). (b) M_{ZFC} and M_{FC} at 5 K, the relative history dependence of magnetization $\Delta M = (M_{\mathrm{FC}} - M_{\mathrm{ZFC}})/M_{\mathrm{ZFC}}(T)$ at 5 K (inset of b). The continuous line is a guide to eye.

expected free-ion value of 3.47 μ_{B} (for 77% of Mn^{3+} and 13% of Mn^{4+}), which indicates that the volume fraction of the ferromagnetic clusters is rather small.

As seen from figure 5, the position of the cusp-like anomaly in $\chi'(T)$ is frequency independent and is associated with the ferromagnetic transition. On lowering the temperature, the ferromagnetic clusters, due to the presence of a random and mixed magnetic interaction, undergo spin freezing. Such a cooperative spin freezing results in a sudden decrease in the χ' signal and a broad shoulder in $\chi'(T)$ (marked by the arrow in figure 5). However, the exact position of the shoulder in $\chi'(T; f)$ and its frequency dependence are rather difficult to determine, and this can be understood as a consequence of the large in-phase component of ac susceptibility associated with ferromagnetism. These observations are in close agreement with the other reports of cobaltate [78] and manganite perovskites [82] exhibiting CG behaviour. It is seen that the dynamic magnetic response changes drastically with the application of bias dc field (figure 6). Overall reduction in the χ' signal and broadening of the transition are observed. While the former is expected to arise when the field saturates the ferromagnetic contribution to the initial susceptibility, the latter might be due to the absence of the long-range ferromagnetic ordering and the slow response of the clusters in the presence of dc field. For

lower fields, the suppression of the χ' signal and broadening of the transitions cause the cusp-like anomaly to appear like a plateau (figure 6(a)). The broad maximum in the $\chi'(T; H)$ curve shifts to lower temperatures for smaller dc fields, i.e., when $H_{dc} \leqslant 0.5$ kOe. For instance, $\chi'(T)$ shows a distinct maximum at ∼58 K when $H_{dc} = 0.25$ kOe, whereas it is found to shift to ∼40 K when the static field is raised to 0.5 kOe. When the field is further increased ($H_{dc} \geqslant 0.75$ kOe), two distinct magnetic transitions, marking the ferromagnetic transition at T_c(∼100 K), followed by spin freezing at $T_g(H)$ (∼28 K) are found. Such a pair of maxima has been observed in other manganites [79, 83] in which the competing magnetic interactions play a dominant role. Another important observation is that the high-temperature maximum shifts towards high temperature and broadens, whereas the low-temperature maximum shifts towards low temperatures with the increase of bias field. The shift of the high-temperature peak to higher temperature and low-temperature peak to lower temperature imply that they are to be associated with FM ordering and spin freezing, respectively. The application of bias field tends to order the spins in the field direction and therefore hinders the randomizing process. Therefore, the shift of the former peak in $\chi'(T; H)$ to higher temperature is the consequence of the partial suppression of magnetic fluctuations, whereas the reduction of the spin-freezing temperature is due to the suppression of the energy barriers with the increasing dc field. Thus the shift of $T_g(H)$ to lower temperatures and the decline of $\chi'(T; H)$ below this temperature together confirm frozen spin-disordered ground state of the compound.

The frequency-dependent susceptibility under bias field ($\chi'(T; H; f)$) provides the details of the spin dynamics associated with the magnetic transitions (figure 8). Under a bias field, no change—either a shift of T_c or suppression of the χ' signal—is observed around the ferromagnetic transition. On the other hand, in the regions very close to and below the spin-freezing transition, the χ' signal shows rather strong frequency dependence. This indicates that while relaxation time effects do not play a major role at T_c, the susceptibility peak at T_g shifts to higher temperature with increasing measuring frequency and the χ' signal declines below this temperature.

As discussed above, the dynamic response of the system indicates a freezing of the moments at low temperatures. In the following, the qualitative features in the ac susceptibility that distinguish the CG, SG and super-paramagnetic (SP) system are discussed. The SG [59, 60, 84] and SP system [85, 86] show only a cusp in the ac susceptibility. The additional features, namely, a broad shoulder and/or a sharp drop of χ' signal at lower temperatures, not only exclude the SG and SP state but also suggest the CG state of the compounds. The dynamic response of the RSG also mimics the CG systems. In the canonical spin-glass systems, the cusp itself shows a frequency-dependent shift to higher temperatures [59, 60]. In a CG, (figure 5) as well as in an RSG, the position of the cusp-like anomaly is frequency independent. The cusp-like anomaly in χ' and the shallow maximum in the ZFC static response of the system are close to each other and are entirely associated with clusters themselves, but not with the SG system, or with the freezing of the magnetic moments. Moreover, in both the RSG and CG, the cusp-like anomaly evolves into two distinct maxima under suitable static bias field, close to T_c and at lower temperatures (T_g), marking the spin-freezing temperature and a decline of χ' below this temperature. Unlike the high-temperature maximum, the latter low-temperature maximum in the χ' signal exhibits a frequency-dependent shift to higher temperatures, one of the characteristic features of both RSG and CG systems. However, based on the intercomparison of the static response of the system under ZFC and FC conditions, it is argued that all compounds of the present investigation show a CG rather than an RSG state.

Quantitative inferences about the glassy ground state can also be obtained from analysis of the frequency dependence of T_g. In all cases, it is found that T_g is linear in the logarithm of frequency, and the normalized slope (p) is taken as a parameter to distinguish between different

glassy systems [79, 87]. Normally, p is estimated in the absence of field [59]. However, as stated earlier, the ferromagnetic and the spin-freezing signals overlap strongly, preventing such an analysis. Hence, p is estimated under a suitable bias field in which the FM and the spin-freezing signals are well separated. The typical value of p (∼0.22) for the compounds is much higher than the typical values for the canonical spin-glass systems ($p \sim 0.005$–0.01) [60] and rare-earth-doped manganites ($p \sim 0.03$–0.05) [79, 82], and is comparable to that of the cobaltates showing a super-paramagnetic-like behaviour [87]. In the present study, the dynamic spin freezing does not follow Arrhenius law, $f = f_0 \exp(-E_a^*/K_B T_g)$, ruling out the super-paramagnetic behaviour of the compounds. Thus, it is concluded from the dynamic studies that the system is not a super-paramagnet, SG or RSG. In conjunction with the static response of the system, it is proposed here that the system exhibits a CG state. It is believed that unusually large value of p in the present case, compared to other reported values of CG system ($p \sim 0.04$) [78], may be due to the giant magnetic moments of ferromagnetic clusters that grow with the application of bias fields.

Slow spin dynamics is another characteristic feature of the glassy ground state. In the present case, the magnetic relaxation represents two different regimes as a function of temperature. The logarithmically slow dynamics is seen not only below the freezing temperature T_g, but also up to T_p, the temperature corresponding to the broad maximum in the $M_{ZFC}(T)$ curves. Above T_p, the relaxation behaviour changes from the logarithmic to purely exponential decay (Debye-like) [88]. This type of magnetic aftereffect, referred to as Richter type, has been observed in bulk and thin-film manganite compounds. These results imply that the ferromagnetic order appearing below T_c is spatially confined; i.e., only clusters of FM order exist below this temperature. This is reinforced by the measurements of $M(H)$ just below T_c (100 K), where Arrot plots (inset of figure 10) show a positive curvature, indicative of a continuous second-order transition [89]. The logarithmic nature of the relaxation is associated with a distribution of energy barriers arising from the random and mixed interactions between the clusters or with time-dependent activation energies. On the other hand, the exponential behaviour is ascribed to the existence of energy barriers opposing cluster growth and reorientation of the cluster moments. The dynamic crossover of logarithmic to exponential behaviour also suggests that the dynamic response above T_p is governed by the clusters, which are aligned with the field, presumably because the reorientation of the non-collinear cluster moments on field cooling is relatively unhindered in this regime. On the other hand, for temperatures below T_p, such cluster moment reorientation may be inhibited and the decay is predominantly due to slowly relaxing anti-aligned clusters.

The magnetic viscosity (S), estimated from the logarithmic relaxation measurements, increases with decreasing temperature. The most striking observation is the two maxima in $S(T)$ curves:; one at ∼40 K, and another at ∼20 K. A maximum in S has also been reported in other magnetic alloys, such as AuFe spin glasses [90], dipolarly interacting frozen ferrofluids [91], and giant magnetoresistive CuCo alloys showing spin-glass like ordering [92]. These studies argue that a maximum results from the competition between two processes: freezing of magnetic moments in the presence of competing magnetic interactions and disorder, and activation of frozen-in moments with increasing temperature. The two maxima in $S(T)$ might be an indication of the presence of a cluster-size distribution as well as of many timescales of relaxation. The low-temperature maximum in the $S(T)$ (∼20 K) curve is just below the frequency-dependent feature in the out-of-phase part of the ac susceptibility (inset of figure 14). It will be shown subsequently that this temperature closely matches that of the broad maximum in the magnetic contribution to the total specific heat of the compound. This supports the idea that the low-temperature maximum in $S(T)$ is related to the freezing of the clusters with large moments. It is interesting to note that at ∼40 K, no anomaly could

be seen either in the zero-field ac susceptibility (figure 5) or in the $M_{ZFC}(T)$ curves (inset of figure 9(c)). It is probable that the maximum at ∼40 K is due to the relaxation of the smaller-size clusters.

In the following, the spin energetics associated with T_g is discussed. The total specific heat measured at zero field (figure 13) shows no evidence for a characteristic λ-type anomaly corresponding to T_c. This is in line with the earlier reports, wherein the anomaly is reported to become broad with diminished height and disappears gradually altogether beyond a certain substitution [14, 55]. This may be due to magnetic inhomogeneity developing within the system. An important property tracking the cluster-glass character is the magnetic contribution to the specific heat (C_{mag}). The $C_{mag}(T)$ curve exhibits a broad maximum just below T_g, very close to the broad shoulder-like feature observed in the zero-field ac susceptibility (figure 5), and closely matches with the low-temperature maximum in the $S(T)$ curve as well. The curve below the maximum exhibits a linear behaviour and the corresponding value of n is ∼1.04 (equation (3)). The system thus shows a linear specific heat below the spin-freezing temperature. Linear temperature dependence of C_{mag} together with the broad maximum close to T_g provides a strong evidence for the cluster-glass state of the compound [60]. Furthermore, an estimate of the magnetic entropy associated with the broad maximum in $C_{mag}(T)$ can be obtained by integrating $\Delta C_{mag}/T$ after subtracting a smooth background (based on a polynomial fit to $C_{mag}(T)$ measured above and below the regions of the peak). The resultant magnetic entropy, S_{mag}, of 1.01 ± 0.02 J mol^{-1} K^{-1} is well below the full spin entropy as expected [62]. From the preceding discussions, it is inferred that the modified magnetic ground state of $La_{0.67}Ca_{0.33}Mn_{0.90}Ta_{0.10}O_3$ compound is a CG state. Based on the intercomparison of the dynamic and static responses of the substituted compounds, it is argued that compounds with $x = 0.05$ and 0.07 of this series also form cluster-glass states.

At this point, the following remarks are pertinent. There are a number of interesting works in recent times that address the issue of the glassy phase of the manganites [89, 93, 94]. These studies have attempted to reanalyse the glassy phase of the compounds in the phase-separation scenario. Recent theoretical works predict the coexistence of clusters in various length scales [6] below a characteristic temperature T^*, and the only theoretical framework with similar characteristics is the phase-separation scenario involving phases with different electron densities or lattice distortions [4]. According to this scenario, it is very likely that the quenched disorder and the competing exchange interactions among the clusters lead to the appearance of locally metastable states. The phase-separated state (PSS), while it does not constitute a conventional spin glass or cluster glass, exhibits many of its features such as time-dependent or frequency-dependent phenomena. And this is the reason that the PSS is often spoken of as a *spin-glass-like* or *cluster-glass-like* state. This issue of phase-separated glassy phase of manganites is currently under discussion, and many more interesting results are expected in the near future. It is expected that the results presented in this paper will attract some attention in future theoretical analyses of the phase-separated glassy state of manganite compounds.

5. Summary

This study demonstrates that pentavalent substitution not only reduces the transition temperatures to the largest extent reported for the Mn-site substituted manganites but also induces glassy behaviour at very low concentration ($x \sim 0.05$) compared to that of other divalent, trivalent or tetravalent substitutions for Mn in the ferromagnetic–metallic $La_{0.67}Ca_{0.33}MnO_3$. Besides modification of majority carrier concentration due to the increased (decreased) Mn^{3+} concentration and enhanced local structural effects, the local electro static

potential due to the deviating charge state of the substituent at the Mn site seems to be certainly important, and it accounts for the unusually strong reduction in the itinerant ferromagnetism of the compounds. Competing magnetic interactions in the background of strong disorder effects modify the ferromagnetic–metallic ground state of CMR manganites. Large thermomagnetic irreversibility just below T_c, a field-dependent broad cusp in the ZFC thermomagnetization and a significant drop of ZFC magnetization below this temperature indicate that the FM state has a short-range order and that it originates from the intra-cluster ferromagnetism. This is also apparent from the non-saturation of magnetization up to a field of 7 T even at 5 K. The glassy feature is revealed by a broad shoulder in the ac susceptibility well below T_c that develops into a separate frequency-dependent peak in the presence of appropriate dc fields. Two distinct magnetic transitions are identified in the ac susceptibility: one close to T_c and the other close to the freezing temperature (T_g). Non-equilibrium spin dynamics with a maximum in the magnetic viscosity close to T_g and a linear low-temperature dependence of magnetic specific heat with a characteristic broad maximum close to T_g support the fact that the modified magnetic ground state of the Ta-substituted $La_{0.67}Ca_{0.33}MnO_3$ is a cluster-glass-like state. Since the issue of a phase-segregated state with glassy characteristics in the ferromagnetic insulating phase is unresolved, the exact mechanism of the cluster-glass state of the compound remains open. Further studies are necessary in this direction.

Acknowledgments

This work is supported by DFG-FOR520, Germany. One of the authors, LSL, also thanks the Council of Scientific and Industrial Research, (CSIR), India, for a Senior Research Fellowship.

References

[1] Tokura Y and Nagosa N 2000 *Science* **288** 462
[2] Cheong S W and Hwang H Y 2000 *Colossal Magnetoresistive Oxides* ed C N R Rao and Y Tokura (India: Gordon and Breach Science Publishers) p 237
[3] Jonker G H and Van Santeen J H 1950 *Physica* **16** 337
[4] Dagotto E, Hotta T and Moreo A 2001 *Phys. Rep.* **344** 1 and references therein
[5] Uehara M, Mori S, Chen C H and Cheong S-W 1999 *Nature* **399** 560
[6] Moreo A, Mayor M, Feiguin A, Yunoki S and Dagotto E 2000 *Phys. Rev. Lett.* **84** 5568
[7] Burgy J, Mayor M, Martin-Mayor V, Moreo A and Dagotto E 2001 *Phys. Rev. Lett.* **87** 277202
[8] Burgy J, Moreo A and Dagotto E 2004 *Phys. Rev. Lett.* **92** 097202
[9] Ahn K H, Wu X W, Liu K and Chien C L 1996 *Phys. Rev.* B **54** 15299
[10] Rubinstein M, Gillespie D J, Snyder J E and Tritt T M 1997 *Phys. Rev.* B **56** 5412
[11] Gayathri N, Raychaudhuri A K, Tiwary S K, Gundakaram R, Arulraj A and Rao C N R 1997 *Phys. Rev.* B **56** 1345
[12] Liu X, Xu X and Zhang Y 2000 *Phys. Rev.* B **62** 15112
[13] Rivadulla F, López-Quintela M A, Hueso L E, Sande P and Rivas J 2000 *Phys. Rev.* B **62** 5678
[14] Awana V P S, Schmitt E, Gmelin E, Gupta A, Narlikar A V, De Lima O F, Cardoso C A, Malik S K and Yelon W B 2000 *J. Appl. Phys.* **87** 5034
[15] Yuan L, Zhu Y and Ong P P 2001 *Solid State Commun.* **120** 495
[16] Sun Y, Tang W and Zhang W 2001 *J. Magn. Magn. Mater.* **231** 195
[17] Deac I G, Tetean R and Burzo E 2007 *J. Magn. Magn. Mater.* **310** 1972
[18] Karnakar S, Taran S, Chaudhuri B K, Sakata H, Sun C P, Huang C L and Yang H D 2006 *Phys. Rev.* B **74** 104407
[19] Turilli G and Licci F 1996 *Phys. Rev.* B **54** 13052
[20] Blasco J, Garcia J, de Teressa J M, Ibarra M R, Perez J, Algarabel P A, Marquina C and Ritter C 1997 *Phys. Rev.* B **55** 8905
[21] Sun Y, Xu X, Zheng L and Zhang Y 1999 *Phys. Rev.* B **60** 12317
[22] Sun J R, Rao G H, Shen B G and Wong H K 1998 *Appl. Phys. Lett.* **73** 2998

[23] Sanchez M C, Blasco J, García J, Stankiewicz J, de Teressa J M and Ibarra M R 1998 *J. Solid State Chem.* **138** 226
[24] Przewoźnik J, Chmist J, Kolwicz-Chodack L, Tarnawski Z, Kołodzieczyk A, Krop K, Kellner K and Gritzner G 2004 *Acta Phys. Pol.* A **106** 665
[25] Wang K Y, Song W H, Dai J M, Ye S L, Wang S G, Fang J, Chen J L, Gao B J, Du J J and Sun Y P 2001 *J. Appl. Phys.* **90** 6263
[26] Seetha Lakshmi L 2006 Mn site substituted $La_{0.67}Ca_{0.33}MnO_3$ ortho-perovskites: role of charge state, local structure and local spin coupling on the ground state properties *PhD Thesis* University of Madras, Chennai, India
[27] Huang Y-H, Liao C-S, Wang Z-M, Li X-H, Yan C-H, Sun J-R and Shen B-G 2002 *Phys. Rev.* B **65** 184423
[28] Yusuf S M, Sahana M, Dörr K, Rößler U K and Müller K-H 2002 *Phys. Rev.* B **66** 064414
[29] Troyanchuk I O, Bushinsky M V, Szymczak H, Bärner K and Maignan A 2004 *Eur. Phys. J.* B **28** 75
[30] De Teresa J M, Ritter C, Ibarra M R, Algarabel P A, García-Muñoz J L, Blasco J, García J and Marquina C 1997 *Phys. Rev.* B **56** 3317
[31] De Teresa J M, Ibarra M R, García J, Blasco J, Ritter C, Algarabel P A, Marquina C and del Moral A 1996 *Phys. Rev. Lett.* **76** 3392
[32] Terai T, Kakeshita T, Fukuda T, Saburi T, Takamoto N, Kindo K and Honda M 1998 *Phys. Rev.* B **58** 14908
[33] Maignan A, Martin C, Van Tendeloo G, Hervieu M and Raveau B 1999 *Phys. Rev.* B **60** 15214
[34] Rodriguez-Martínez L M and Attfield J P 2000 *Phys. Rev.* B **63** 024424
[35] Nair S and Banerjee A 2004 *Phys. Rev. Lett.* **93** 117204
[36] Wu B-M, Li B, Zhen W-H, Ausloos M, Du Y-L, Fagnard J F and Vanderbemden Ph 2005 *J. Appl. Phys.* **97** 103908
[37] Cai J-W, Wang C, Shen B-G, Zhao J-G and Zhan W-S 1997 *Appl. Phys. Lett.* **71** 1727
[38] Yusuf S M, Sahana M, Hegde M S, Dörr K and Müller K-H 2000 *Phys. Rev.* B **62** 1118
[39] Dagotto E 2005 *New J. Phys.* **7** 67
[40] Seetha Lakshmi L, Sridharan V, Natarajan D V, Sastry V S and Radhakrishnan T S 2001 *Pramana J. Phys.* **58** 1019
[41] Seetha Lakshmi L, Sridharan V, Natarajan D V, Rawat R, Chandra S, Sastry V S and Radhakrishnan T S 2004 *J. Magn. Magn. Mater.* **279** 41
[42] Seetha Lakshmi L, Dörr K, Nenkov K, Sridharan V, Sastry V S and Müller K-H 2007 *J. Phys.: Condens. Matter* at press
[43] Seetha Lakshmi L, Dörr K, Nenkov K, Sridharan V, Sastry V S and Müller K-H 2005 *J. Magn. Magn. Mater.* **290/291** 924
[44] Larson A C and von Dreele R B 2000 *Los Alamos National Laboratory Report LAUR* pp 86–748
[45] Lufaso M W and Woodward P M 2001 *Acta Crystallogr.* B **57** 725
[46] Hwang J S, Lin K and Tien C 1997 *Rev. Sci. Instrum.* **68** 94
[47] Bontemps N and Orbach R 1988 *Phys. Rev.* B **37** 4708
[48] Škorvánek I, Skwirblies S and Kötzler J 2001 *Phys. Rev.* B **64** 1884437
[49] Laiho R, Lisunov K G, Lähderanta E, Petrenko P, Salminen J, Stamov V N and Zakhvalinskii V S 2000 *J. Phys.: Condens. Matter* **12** 5751
[50] Deac I G, Diaz S V, Kim B G, Cheong S-W and Schiffer P 2002 *Phys. Rev.* B **65** 174426
[51] Mathieu R, Nordblad P, Nam D N H, Phuc N X and Khiem N V 2001 *Phys. Rev.* B **63** 174405
[52] Müller K-H 2001 *Encyclopedia of Materials: Science and Technology* vol 5, ed K-H J Buschow, R W Cahn, M C Flemings, B Ilschner, E J Kramer and S Mahajan (Amsterdam: Elsevier) pp 4997–5004 (ISBN:0-08-0431526)
[53] Aharoni A 1992 *Phys. Rev.* B **46** 5434
[54] Lin P, Chun S H and Salamon M B 2000 *J. Appl. Phys.* **87** 5825
[55] Rao G H, Sun J R, Kattwinkel A, Haupt L, Bärner K, Schmitt E and Gmelin E 1999 *Physica* B **269** 379
[56] Rößler S, Rößler U K, Nenkov K, Eckert D, Yusuf S M, Dörr K and Müller K-H 2004 *Phys. Rev.* B **70** 104417
[57] Gopal E S R 1966 *Specific Heat at Low Temperatures* (New York: Plenum)
[58] Woodfield B F, Wilson M L and Byers J M 1997 *Phys. Rev. Lett.* **78** 3201
[59] Binder K and Young A P 1986 *Rev. Mod. Phys.* **58** 801
[60] Mydosh J A 1993 *Spin Glasses; An Experimental Introduction* (London: Taylor and Francis)
[61] Löhneysen H v, van den Berg R, Lecomte G V and Zinn W 1985 *Phys. Rev.* B **31** 2920
[62] Ghivelder L, Abrego Castillo I, Alford N McN, Tomka G J, Riedi P C, MacManus-Driscoll J, Akther Hossain A K M and Cohen L F 1998 *J. Magn. Magn. Mater.* **189** 274
[63] Sahana M, Dörr K, Doerr M, Eckert D, Müller K-H, Nenkov K, Schultz L and Hegde M S 2000 *J. Magn. Magn. Mater.* **213** 253

[64] Nam D N H, Mathieu R, Nordblad P, Khiem N V and Phuc N X 2000 *Phys. Rev.* B **62** 1027
[65] Woo H, Tyson T A, Croft M and Cheong S-W 2004 *J. Phys.: Condens. Matter* **16** 2689
[66] Dho J, Kim W S and Hur N H 2002 *Phys. Rev. Lett.* **89** 027202
[67] Sun Y, Xu X, Tong W and Zhang Y 2000 *Appl. Phys. Lett.* **77** 2734
[68] Wang Z-H, Shen B-G, Tang N, Cai J-W, Ji T-H, Che G-C, Dai S-Y and Ng D H L 1999 *J. Appl. Phys.* **85** 5399
[69] Li R-W, Wang Z-H, Chen X, Sun J-R, Shen B-G and Yan C-H 2000 *J. Appl. Phys.* **87** 5597
[70] von Helmolt R, Haupt L, Bärner K and Sondermann U 1992 *Solid State Commun.* **82** 693
[71] Haupt L, Von Helmolt R, Sondermann U, Bärner K, Tang Y, Giessinger E R, Ladizinsky E and Braunstein R 1992 *Phys. Lett.* A **165** 473
[72] Itoh M, Natori I, Kubota S and Motoya K 1994 *J. Phys. Soc. Japan* **63** 1486
[73] Moritomo Y, Tomioka Y, Asamitsu A, Tokura Y and Matsui Y 1995 *Phys. Rev.* B **51** 3297
[74] Abdul-Razzaq W and Kouvel J S 1987 *Phys. Rev.* B **35** 1764
[75] Ando T, Ohta E and Sato T 1996 *J. Magn. Magn. Mater.* **163** 277
[76] Abdul-Razzaq W, Kouvel J S and Claus H 1984 *Phys. Rev.* B **30** 6480
[77] Kaul S N and Srikanth S 1998 *J. Phys.: Condens. Matter* **10** 11067
[78] Mukherjee S, Ranganathan R, Anilkumar P S and Joy P A 1996 *Phys. Rev.* B **54** 9267
[79] Deac I G, Mitchell J F and Schiffer P 2001 *Phys. Rev.* B **63** 172408
[80] Chikazumi S 1997 *Physics of Ferromagnetism* (Oxford: Clarendon)
[81] Nagamine L C C M, Mevel B, Dienty B, Rodmacq B, Regnard J R, Revenant-Brizard C and Manzini I 1999 *J. Magn. Magn. Mater.* **195** 437
[82] Freitas R S, Ghivelder L, Damay F, Dias F and Cohen L F 2001 *Phys. Rev.* B **64** 144404
[83] Sahana M, Venimadhav A, Hegde M S, Nenkov K, Rößler U K, Dörr K and Müller K-H 2003 *J. Magn. Magn. Mater.* **263** 361
[84] Mulder C A M, van Duyneveldt A J and Mydosh J A 1981 *Phys. Rev.* B **23** 1384
[85] Dormann J L, Cherkaoui R, Spinu L, Noguès M, Lucari F, Orazio F D, Fiorani D, Garcia A, Tronc E and Jolivet J P 1998 *J. Magn. Magn. Mater.* **187** L139
[86] Lue C S, Ross J H Jr, Rathnayaka K D D, Naugle D G, Wu S Y and Li W-H 2001 *J. Phys.: Condens. Matter* **13** 1585
[87] Mahendiran R, Bréard Y, Hervieu M, Raveau B and Schiffer P 2003 *Phys. Rev.* B **68** 104402
[88] Sirena M, Steren L B and Guimpel J 2001 *Phys. Rev.* B **64** 104409
[89] Rivadulla F, Rivas J and Goodenough J B 2004 *Phys. Rev.* B **70** 172410
[90] Guy C N 1978 *J. Phys. F: Met. Phys.* **8** 1309
[91] Luo W, Nagel S R, Rosenbaum T F and Rosensweig R E 1991 *Phys. Rev. Lett.* **67** 2721
[92] Idzilkowski B, Rößler U K, Eckert D, Nenkov K and Müller K-H 1999 *Europhys. Lett.* **45** 714
[93] Rivadulla F, López-Quintela M A and Rivas J 2004 *Phys. Rev. Lett.* **93** 167206
[94] Rivas J, Rivadulla F and López-Quintela M A 2004 *Physica* B **354** 1